The Astronomical Journal, 133:2008–2014, 2007 May

MEASURING THE MASS OF A PRE-MAIN-SEQUENCE BINARY STAR THROUGH THE ORBIT OF TWA 5A

Q. M. Konopacky,[1,2] A. M. Ghez,[1,2] G. Duchêne,[3] C. McCabe,[4] and B. A. Macintosh[5]

Received 2005 September 16; accepted 2007 January 18

ABSTRACT

We present the results of a 5 yr monitoring campaign of the close binary TWA 5Aab in the TW Hydrae association, using speckle and adaptive optics on the W. M. Keck 10 m telescopes. These measurements were taken as part of our ongoing monitoring of pre-main-sequence (PMS) binaries in an effort to increase the number of dynamically determined PMS masses and thereby calibrate the theoretical PMS evolutionary tracks. Our observations have allowed us to obtain the first determination of this system's astrometric orbit. We find an orbital period of 5.94 ± 0.09 yr and a semimajor axis of $0.066'' \pm 0.005''$. Combining these results with a kinematic distance, we calculate a total mass of $0.71 \pm 0.14\ M_{\odot}(D/44\ \mathrm{pc})^3$ for this system. This mass measurement, as well as the estimated age of this system, is consistent to within 2 σ of all theoretical models considered. In this analysis we properly account for correlated uncertainties, and we show that while these correlations are generally ignored, they increase the formal uncertainties by up to a factor of 5 and therefore are important to incorporate. With only a few more years of observation, this type of measurement will allow the theoretical models to be distinguished.

Key words: binaries: visual — stars: fundamental parameters — stars: individual (TWA 5A) — stars: pre–main-sequence

1. INTRODUCTION

Binary stars present a unique laboratory for the study of stellar evolution, as their orbital solutions give direct mass estimates. Although the mass of a star is the most fundamental parameter in determining its course of evolution, very few pre-main-sequence (PMS) stars have dynamically determined masses. In these few cases, astrometric and spectroscopic studies have lead to PMS mass determinations based on the orbital motion of a stellar companion or a circumstellar disk relative to the primary star (e.g., Ghez et al. 1995; Simon et al. 2000; Steffen et al. 2001; Woitas et al. 2001; Tamazian et al. 2002; Duchêne et al. 2003). Once measured, these masses can subsequently be used to constrain PMS evolutionary models. These models have been shown to be systematically discrepant in their predictions by up to factors of 2 in mass and 10 in age; still, since there are so few well-determined PMS masses, little can currently be done to calibrate these tracks. This is particularly true in the lowest mass regime, where only three systems have total dynamical masses of less than 1 $M_{\odot}$ and only one single star has a dynamical mass measurement below 0.5 $M_{\odot}$ (Hillenbrand & White 2004). This study is part of an ongoing program to astrometrically determine the orbits of PMS stars and to help constrain these theoretical mass tracks. Young stars are particularly important to correctly calibrate, as this calibration will aid in the subsequent calibration of young brown dwarf and planetary models.

The TW Hydrae association was originally discovered by Kastner et al. (1997), with only five members confirmed at that time. Since its discovery, 25 total members have been identified (e.g., Song et al. 2003; Makarov & Fabricius 2001). The association has been shown to be quite young (~8–12 Myr) via lithium abundance tests, space motions, and placement of its members on the H-R diagram (e.g., Zuckerman & Song 2004). In addition, TW Hydrae is quite nearby, with an average distance of ~50 pc (e.g., Makarov & Fabricius 2001; Mamajek 2005). This makes TW Hydrae one of the closest associations of young stars to the Earth and thus an ideal region for studying spatially resolved PMS binaries, as they are likely to have orbital periods as short as a few years.

With these ideas in mind, we began to monitor TWA 5, the fifth of the five original members of the TW Hydrae association identified by Kastner et al. (1997). TWA 5 is composed of at least three components. The pair that we analyze here is TWA 5Aa-Ab, which had a separation of ~0.06″ when it was discovered by Macintosh et al. (2001). TWA 5A also has a brown dwarf companion, TWA 5B, located ~2″ away (Webb et al. 1999; Lowrance et al. 1999; Neuhäuser et al. 2000; Mohanty et al. 2003). Finally, TWA 5Aab is suspected to contain at least one spectroscopic pair based on large radial velocity variations (Torres et al. 2003; G. Torres 2005, private communication).

In this paper we present the results of 5 yr of speckle and adaptive optics (AO) observations of TWA 5Aab with the W. M. Keck 10 m telescopes. In § 2 we describe our data reduction techniques, and in § 3 we present our orbital solution for the system. In § 4 we discuss comparisons of our derived orbital parameters with mass and age predictions from theoretical PMS tracks and make recommendations for future studies of this system.

2. OBSERVATIONS AND DATA ANALYSIS

2.1. *Speckle Data*

TWA 5Aab was observed using the Keck I 10 m telescope with the facility's Near Infrared Camera (NIRC; Matthews & Soifer 1994; Matthews et al. 1996) roughly once a year from 2001 to 2005 (see Table 1 for exact dates). In its high angular resolution mode, NIRC has a pixel scale of 20.44 ± 0.03 mas pixel^{-1} (see the Appendix for details of NIRC's pixel scale and orientation). Three to four stacks of 190 images, each 0.137 s long, were

[1] Division of Astronomy and Astrophysics, University of California, Los Angeles, CA 90095-1547, USA; quinn@astro.ucla.edu, ghez@astro.ucla.edu.
[2] Institute of Geophysics and Planetary Physics, University of California, Los Angeles, CA 90095-1565, USA.
[3] Laboratoire d'Astrophysique, Observatoire de Grenoble, Universite Joseph Fourier, Grenoble Cedex 9, France; gaspard.duchene@obs.ujf-grenoble.fr.
[4] NASA Jet Propulsion Laboratory, Pasadena, CA 91109-8099, USA; mccabe@jpl.nasa.gov.
[5] Institute of Geophysics and Planetary Physics, Lawrence Livermore National Laboratory, Livermore, CA 94551, USA; bmac@igpp.ucllnl.org.

TABLE 1
TWA 5A Binary Star Parameters

Date of Observation	Filter	λ_0 (μm)	Separation (arcsec)	Position Angle (deg)	Flux Ratio (Aa/Ab)	Speckle or AO?	Reference
2000 Feb 20	H	1.648	0.0548 ± 0.0005	205.9 ± 1.0	1.09 ± 0.02	AO	2
2000 Feb 22	K'	2.127	0.054 ± 0.003	204.2 ± 3.0	1.11 ± 0.07	AO	3
	H	1.648	...	...	1.09 ± 0.08	AO	3
	J	1.26	...	...	0.94 ± 0.05	AO	3
2001 May 6	K	2.2	0.0351 ± 0.0002	12.67 ± 1.06	1.26 ± 0.09	Sp	1
2002 May 23	K	2.2	0.013 ± 0.003	313.66 ± 2.99	1.24 ± 0.08[a]	Sp	1
2003 Dec 5	K	2.2	0.0306 ± 0.0004	227.41 ± 5.49	1.22 ± 0.04	Sp	1
2004 Dec 18	K	2.2	0.0515 ± 0.0009	32.10 ± 2.22	1.39 ± 0.09	Sp	1
2005 Feb 16	Fe II	1.65	0.053 ± 0.001	32.59 ± 5.22	1.29 ± 0.18	AO	1
2005 May 27	K	2.2	0.0574 ± 0.0003	29.68 ± 0.35	1.23 ± 0.04	Sp	1
2005 Dec 12	Kp	2.124	0.0571 ± 0.001	29.99 ± 2.26	1.10 ± 0.05	AO	1
	H	1.633	0.0571 ± 0.002	28.89 ± 0.99	1.09 ± 0.03	AO	1
	J	1.248	0.0568 ± 0.005	28.41 ± 3.15	1.05 ± 0.13	AO	1

[a] Flux ratio fixed in this epoch.
References.—(1) This work; (2) Macintosh et al. 2001; (3) Brandeker et al. 2003.

obtained through the K bandpass filter ($\lambda_0 = 2.2$ μm, $\Delta\lambda = 0.4$ μm). They were taken in stationary mode, meaning the Keck pupil is fixed with respect to the detector during the observations but the sky rotates. The rotation rate is sufficiently slow that it is negligible for individual exposures but not over the entire stack. Stacks of four dark frames were also taken with each object stack. In addition, identical stacks of a point source calibrator star (TWA 1 for the 2001–2002 observations and TWA 7 for the 2003–2005 observations) and an empty portion of sky were obtained immediately before or after the target stacks.

The stacks were processed using image reduction and speckle data analysis techniques. Specifically, each image was first dark- and sky-subtracted and flat-fielded, and bad pixels were repaired. The images were then individually corrected for a minor optical distortion in NIRC (J. Lu et al. 2007, in preparation). The object, calibrator, and sky stacks were then Fourier transformed and squared to obtain stacks of power spectra. Next, the calibrator stacks and sky stacks were each averaged together (without rotation). The extraction of the object's intrinsic power spectra used the convolution theorem, which gave the relation

$$O = \frac{I - \langle S \rangle}{\langle C \rangle - \langle S \rangle}, \quad (1)$$

where O is the object power spectrum, I is the initial squared Fourier transform of the object, $\langle S \rangle$ is the averaged, squared power spectrum of the sky, and $\langle C \rangle$ is the averaged, squared power spectrum of the calibrator. Each power spectrum of the object was then rotated so that north is up; these rotated power spectra were combined to obtain an average power spectrum for the stack. Finally, those individual stacks were also averaged together to produce a final power spectrum. This sequence is necessary due to the lack of azimuthal symmetry of the Keck I pupil.

Since a binary star in the image domain is essentially two delta functions, the power spectra can be approximated as a sinusoid with the functional form

$$P(\boldsymbol{f}) = \frac{R^2 + 1 + 2R\cos(2\pi \boldsymbol{f} \cdot \boldsymbol{s})}{R^2 + 1 + 2R}, \quad (2)$$

where R is the flux ratio of the binary star and $\boldsymbol{s}$ is the vector separation of the two stars. This function is fit to our two-dimensional power spectra over all spatial frequencies from 2.68 to 17.6 arcsec^{-1} (this procedure is described in detail in Ghez et al. 1995). The lower cutoff is imposed to avoid spatial frequencies that are corrupted by small changes in the atmospheric conditions between the object and the calibrator, whereas the upper cutoff is imposed to reject excess noise at the highest spatial frequencies. This fitting procedure gives a very accurate estimate of the binary star's separation and flux ratio for components separated by more than $\lambda/2D$, leaving only a 180° position angle ambiguity. This ambiguity is resolved by reanalyzing the original images using the method of shift and add. The brightest speckle in the speckle cloud in each image of the stack is shifted to a common position, and then all the images are added together to produce a diffraction-limited core surrounded by a large, diffuse halo. These images allow us to determine the correct orientation of the position angles of TWA 5A. In one epoch (2002), the binary separation was less than $\lambda/2D$, and hence the first minimum of the power spectrum was not measured; without this measurement, the separation and the flux ratio are degenerate. For this epoch, we fix the flux ratio to the weighted average of the K-band flux ratio measurements of all the other epochs and fit only the separation, as there is no evidence of statistically significant photometric variability over the course of our observations. Uncertainties for all parameters are determined by fitting each of the individual, stack-averaged images that contribute to the final image by the same procedure, and then taking the rms of those values with respect to the average value; for the 2002 epoch we also account for the uncertainty in the weighted-average flux ratio, which is taken to be the rms of the individual K-band flux ratio measurements at all other epochs.

2.2. *Adaptive Optics Data*

TWA 5Aab was also observed using the Keck II 10 m telescope with the AO system (Wizinowich et al. 2000) and the facility's near-infrared camera, NIRC2 (K. Matthews et al. 2007, in preparation), on 2005 February 16 and again on 2005 December 12. For these measurements, we used observations of the Galactic center to establish that NIRC2's narrow camera (which we used) has a plate scale of 9.961 ± 0.007 mas pixel^{-1} and columns that are at a position angle of −0.015° ± 0.134° relative to north (J. Lu et al. 2007, in preparation). In February five images, each of 0.2 s exposure time and 30 co-additions, were taken through the Fe II narrow bandpass filter ($\lambda_0 = 1.65$ μm, $\Delta\lambda = 0.03$ μm).

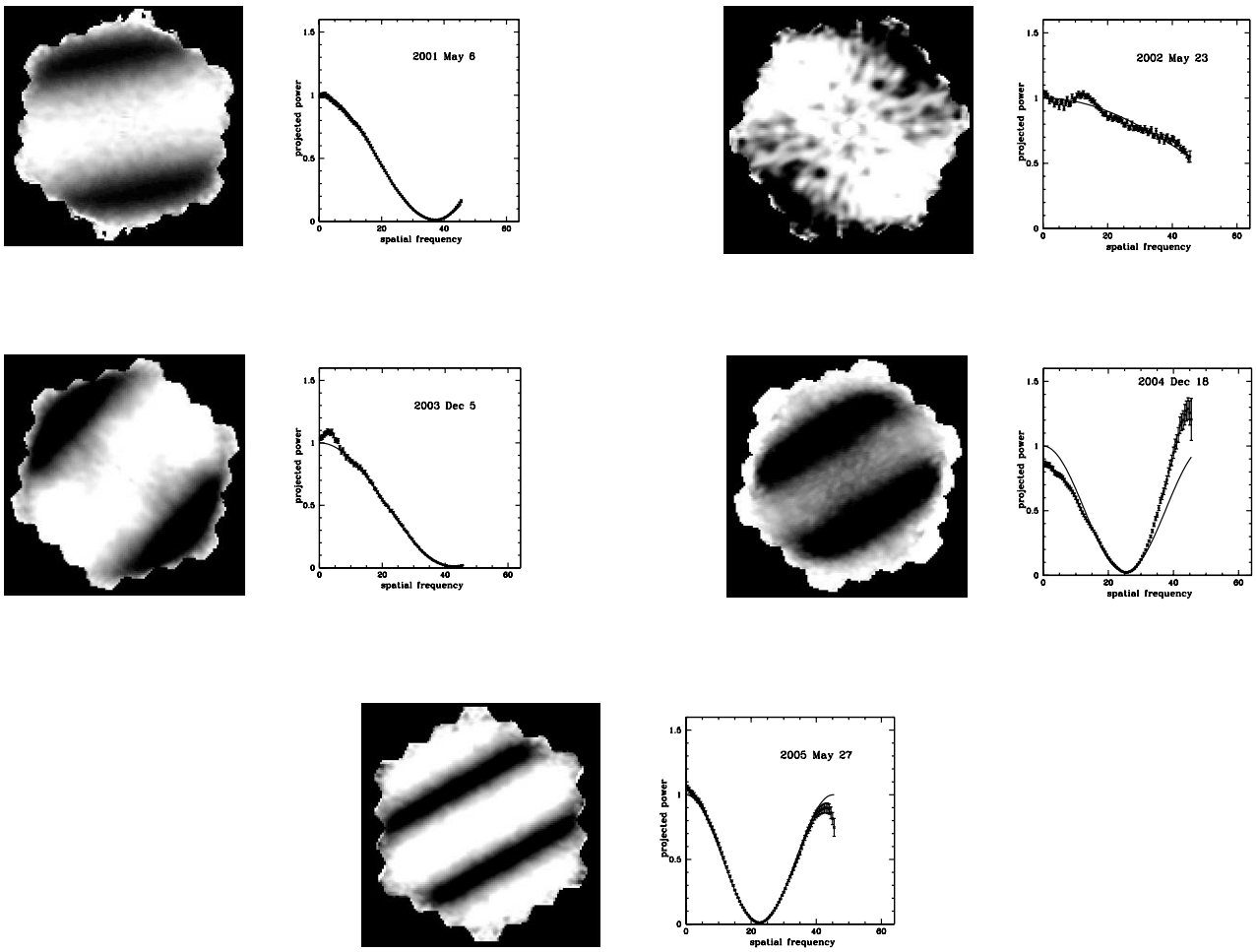

FIG. 1.—Two-dimensional visibilities for all speckle data shown in combination with plots of one-dimensional cuts through the visibilities. The data points represent actual data, while the solid lines show the best fit of eq. (1) to these data. The data from 2002 clearly illustrate that the separation of the binary during this epoch was below the diffraction limit. The degeneracy of the separation and flux ratio in this fit (where the first minimum was not reached) necessitated the fixing of the flux ratio in this epoch to obtain the correct separation. The results of this analysis can be seen in Fig. 3. The slight discrepancy in the 2004 fit comes from a discrepancy between the calibrator and the object, stemming from large-scale changes in seeing on short timescales. However, the large error bars on this data point account for this variation, and thus they do not weigh heavily in our orbital fit.

In December six, six, and three images of 0.181 s exposure time and 50 co-additions were taken through the J ($\lambda_0 = 1.248$ μm, $\Delta\lambda = 0.163$ μm), H ($\lambda_0 = 1.633$ μm, $\Delta\lambda = 0.296$ μm), and K' ($\lambda_0 = 2.124$ μm, $\Delta\lambda = 0.351$ μm) bandpass filters, respectively. These images were processed using the same standard data reduction techniques listed above and then shifted and combined to produce a final image.

Astrometry and flux ratios were then obtained using the IDL package StarFinder (Diolaiti et al. 2000). The wide brown dwarf companion to the system, TWA 5B, was visible in all AO images taken and thus was used as the empirical point-spread function required by the StarFinder fitting algorithm. Both components of the close binary were successfully fit by StarFinder in all cases. Errors were calculated by fitting the components in all individual images that contributed to the combined images and finding the rms of the values derived therein.

3. RESULTS

Figure 1 shows the calibrated power spectra and our resulting fits for all five speckle measurements of TWA 5Aab, and Figure 2 displays our 2005 AO images. We supplement our observations with the following measurements that also spatially resolve TWA 5Aab: the original discovery measurement by Macintosh et al. (2001) and another taken 2 days later by Brandeker et al. (2003). Table 1 lists all separation, position angle, and flux ratio measurements used in this study.

Over the 6 yr that the components of TWA 5A have been spatially resolved, the binary has undergone a full orbit (see Fig. 3), allowing an accurate estimate of its orbital parameters. We calculate an orbital solution for TWA 5A using the Thiele-Innes method (e.g., Hilditch 2001), minimizing the χ^2 between the model and the measurements, which are converted from angular separation and position angle to right ascension and declination. Our model incorporates the following seven standard orbital elements: P (period), A (semimajor axis), e (eccentricity), i (inclination), T_0 (time of periapse passage), Ω (longitude of ascending node), and ω (argument of pericenter). With nine two-dimensional astrometric measurements, there are 11 degrees of freedom in our fit. The best-fitting model produced a χ^2 of 8.91 with 11 degrees of freedom. Furthermore, of the nine data points used in the fit, seven are within 1 σ and two are within 2 σ of the model, suggesting that our fit is good. The 1 σ uncertainties in the model parameters are estimated by changing the values of χ^2 by 1 (Bevington & Robinson 1992). Table 2 lists the best-fit orbital parameters and their uncertainties, and Figure 3 shows our solution for the projected orbit of TWA 5A. This astrometric solution

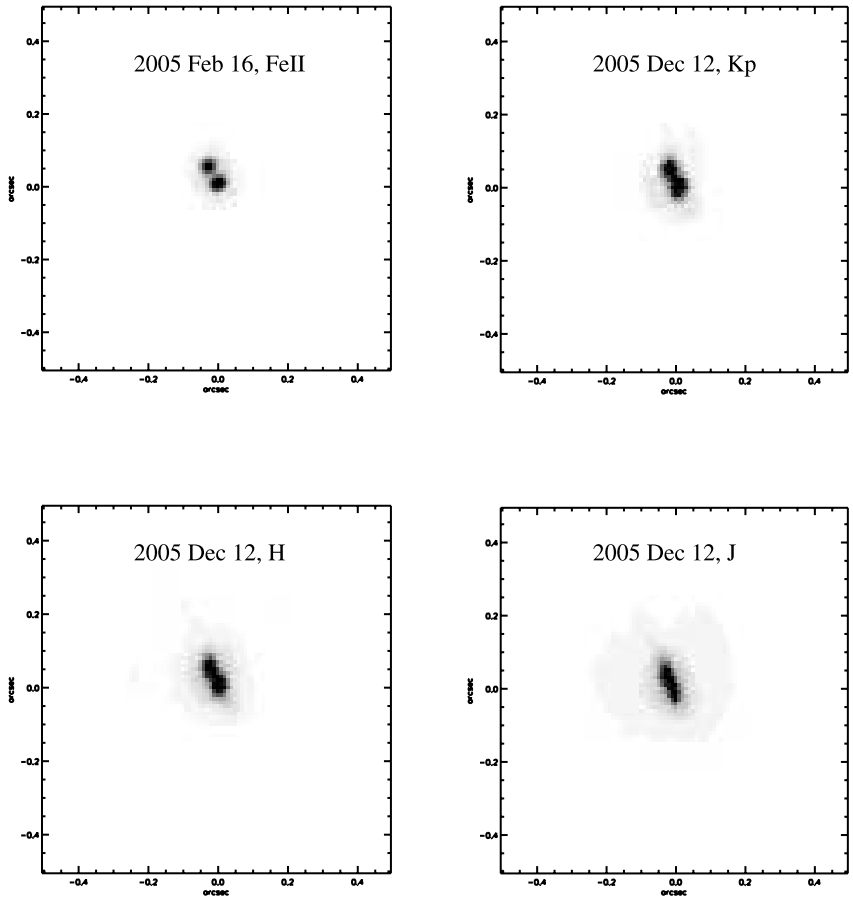

FIG. 2.—NIRC2 AO images of TWA 5A taken on 2005 February 16 and December 12. In all images, north is up, and east is to the left. Component TWA 5Aa is to the southwest, and component TWA 5Ab is to the northeast.

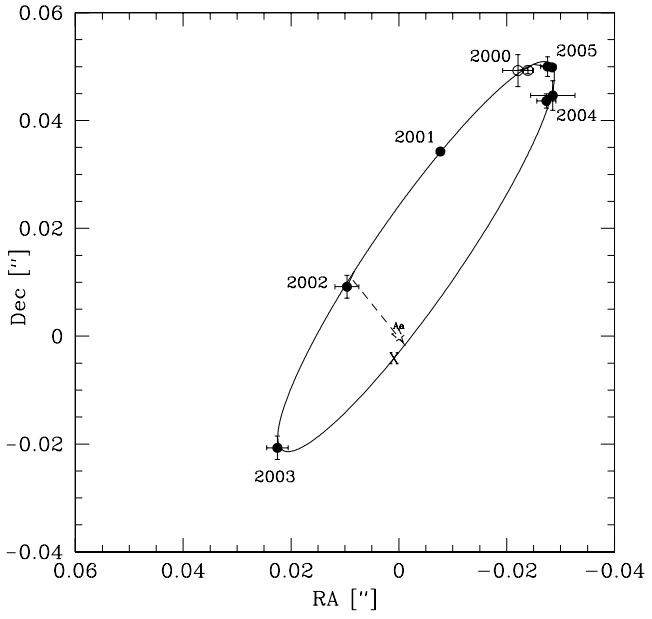

FIG. 3.—Orbital solution for TWA 5Aa and TWA 5Ab. The filled circles represent the data from this study, while the open circles represent the data taken from the literature (both in 2000). The star at [0, 0] marks the position of TWA 5Aa; the lines from the data points to the ellipse indicate where the fit believes the point should lie on the orbit. The dashed line represents the line of nodes, and the cross marks the location of closest approach. The parameters for this orbit are given in Table 2.

yields a mass of $0.71 \pm (0.14 \pm 0.19)\,M_{\odot}$, where the two sources of uncertainty stem from our orbital solution and the 9% uncertainty in the kinematic distance estimate to TWA 5A (Mamajek 2005).

4. DISCUSSION AND CONCLUSIONS

With a well-determined astrometric orbit for TWA 5A, it is possible to begin to compare dynamical estimates of mass with those inferred from theoretical PMS tracks. By comparing the quantity $M/(D/44\ \mathrm{pc})^3$, we preserve the high precision of the astrometric data in the analysis. Here we investigate the models by Baraffe et al. (1998; $\alpha = 1.0$), D'Antona & Mazzitelli (1997), Palla & Stahler (1999), Siess et al. (2000), and Swenson et al. (1994).

TABLE 2
ORBITAL PARAMETERS OF TWA 5A

Parameter	Value
P (yr)	5.94 ± 0.09
A (arcsec)	0.066 ± 0.005
T_0 (yr)	2004.34 ± 0.09
e	0.78 ± 0.05
i (deg)	97.4 ± 1.1
Ω (deg)	37.4 ± 0.9
ω (deg)	255 ± 3

NOTE.—We note that the value of Ω is actually subject to a 180° ambiguity without three-dimensional velocity information.

TABLE 3
TWA 5 System Photometry

Component	Spectral Type	m_K	m_H	m_J	$J-H$	$H-K$	log(Temp.) (K)	log(Lum.) ($L_\odot$)
TWA 5Aa.....	M1.5 ± 0.5	7.39 ± 0.04	7.69 ± 0.04	8.40 ± 0.07	0.71 ± 0.08	0.30 ± 0.06	3.56 ± 0.01	−0.80 ± 0.08
TWA 5Ab.....	[M1.5 ± 0.5]	7.62 ± 0.08	7.79 ± 0.05	8.45 ± 0.15	0.66 ± 0.16	0.17 ± 0.09	3.56 ± 0.01	−0.84 ± 0.08

Notes.—The apparent *K*-, *H*-, and *J*-band magnitudes for TWA 5Aa and 5Ab are computed using 2MASS measurements of the combined magnitudes and the flux ratio measurements given in Table 1. For the *H* and *J* bands we use the most recent AO flux ratio measurements taken with NIRC2 in 2006 December. For the *K* band we use the average flux ratio from all speckle measurements (excluding the unresolved measurement in 2002). The spectral type for TWA 5Ab is assumed to be roughly the same as that for TWA 5Aa, given that the two components have nearly equal brightness. Temperatures are estimated from the scalings given in Luhman et al. (2003), while bolometric luminosities are calculated using the kinematic distance and *H*-band bolometric corrections (K. L. Luhman 2005, private communication).

Model estimates of mass and age require both effective temperature and bolometric luminosity as inputs. Effective temperatures are estimated from the unresolved spectral type for TWA 5A and component flux ratios. The photometric analysis performed here and elsewhere (see Table 1) shows that the two components of TWA 5A have nearly equal brightness out to 1.6 μm. We therefore assume that the components have the same spectral type and assign it to be M1.5 ± 0.5, the spectral type found from a spatially unresolved spectrum (Webb et al. 1999). This is consistent with the $J-H$ colors for each component, which are calculated by combining the Two Micron All Sky Survey (2MASS) unresolved magnitudes with the flux ratios measured here [$J-H(\mathrm{M1.5}) = 0.67$; Leggett 1992]. We estimate the temperature of these components using a conversion of spectral type to effective temperature given in Luhman et al. (2003). These temperatures are intermediate between dwarf and giant stars, thus making them appropriate for PMS stars like TWA 5A. Bolometric luminosities are estimated using our *H*-band magnitudes and the corresponding *H*-band bolometric corrections for PMS stars (K. L. Luhman 2005, private communication), along with the kinematic distance for TWA 5A of 44 ± 4 pc (Mamajek 2005). These input values are given in Table 3.

The uncertainties in $M/(D/44\ \mathrm{pc})^3$ and age from each model are estimated through Monte Carlo simulations. Our Monte Carlo simulation was run with 10^5 points sampled from random, independent Gaussian distributions of *H*-band flux densities and flux density ratios, temperatures for each component, and distance. This allowed us to correctly account for the correlation between input values. In particular, the bolometric correction used for determining the luminosity stems from the effective temperature. In addition, the luminosities of the primary and the secondary are correlated, as they are calculated from the same parameters, namely, the total flux and the flux ratios. Each of these values were converted into sets of temperatures and bolometric luminosities, which were fed into the models to produce estimates of masses and ages for each component. Using the distance assumed for each run, we converted the total mass of both components to $M/(D/44\ \mathrm{pc})^3$. We emphasize that although the predictions of the models are clearly not independent of the distance uncertainty, by using this quantity as opposed to the total mass, we can leave the distance uncertainty out of our dynamical measurement. Thus, we generate contours that correctly represent the 1 σ uncertainties on the masses and ages derived from the model tracks.

Figure 4 shows the dynamical mass normalized by the distance cubed and with it the estimated age of the TW Hydrae association (10 ± 2 Myr, based on comparison with the β Pictoris moving group; Zuckerman & Song 2004), compared with the model predictions as determined by the Monte Carlo simulations. While the input values are generally treated as independent variables, the Monte Carlo simulations demonstrate that it is important to consider the existing correlations between input values, as the resulting uncertainties are otherwise significantly underestimated (by up to a factor of 5, depending on the model). With this proper treatment, the dynamical mass and age estimates are within 2 σ of all five tracks.

While it is reassuring that current models agree with these measurements, we are unable to distinguish between the model tracks. Future improvements in the precision of both the distance and the temperature would allow for a more illuminating comparison between the theoretical models. The temperature uncertainties on the components of TWA 5A could be substantially reduced with spatially resolved spectral types, which should drive the uncertainty in the temperature down to $\pm\frac{1}{4}$ of a spectral subclass. Uncertainties in the distance could also be substantially reduced. Typical uncertainties in new parallax measurements are on the order of a few milliarcseconds, with improvements on these results promised in the near future (Vrba et al. 2004). A separate method to determine the distance is the addition of

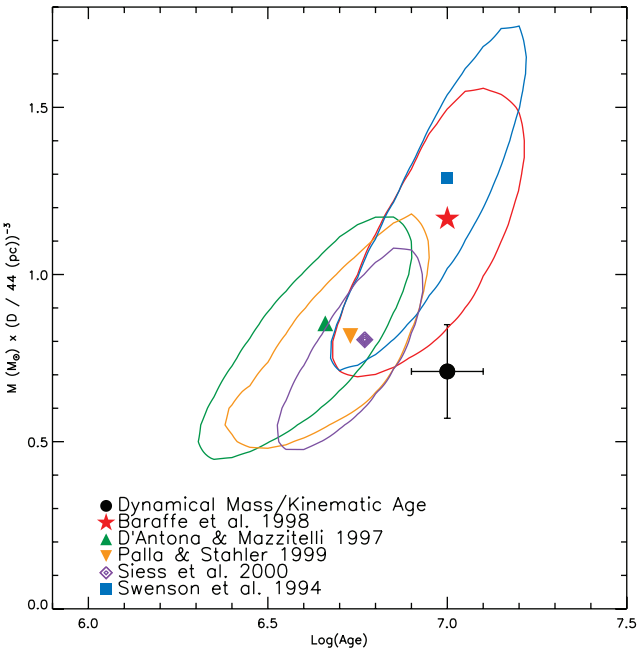

Fig. 4.—Mass and age for TWA 5Aab calculated from the dynamical solution and predicted from each of the five theoretical models considered. The age shown here is the age predicted for the primary, but the age predictions for both components are consistent with each other. The masses are divided by the distance cubed. Although the predictions of the models do include the distance uncertainty, by using the quantity $M/(D/44\ \mathrm{pc})^3$, we ensure that only the model contours are affected by distance uncertainty, avoiding correlation between the models and our dynamical measurement.

spatially resolved radial velocities, which would allow an independent distance estimate from the orbital parameters. In principle, a factor of 2 improvement in the distance uncertainty could be achieved. These radial velocity measurements would also improve the total mass estimate, as would additional astrometric measurements, and would also eventually allow for the determination of *individual* masses of each of the components. However, a potential complication is the possible existence of an additional component in the system (Torres et al. 2003). Another possible method of determining the individual masses of the components of TWA 5A is to use absolute astrometry with respect to TWA 5B, as was done recently for T Tau S (Duchêne et al. 2006). If we just take the improvements expected from future parallax measurements, spatially resolved spectra, and additional astrometry, we expect to be able to distinguish between the tracks at the $\sim 3\ \sigma$ level.

Future spatially resolved spectral types would also address the marginal inconsistency between the $J - H$ and $H - K$ colors for the primary. Currently, we have assumed that this arises from a small K-band excess ($2\ \sigma$). Torres et al. (2003) suggest that an additional component may be present in the system. If this component were particularly low mass, it could give rise to the apparent K-band excess of the primary. Alternatively, the infrared excess could arise from circumstellar material. Mohanty et al. (2003) report the detection of strong Hα emission in an unresolved, high-resolution spectrum of TWA 5A, implying that at least one of the components is accreting. However, no mid-infrared excess has been detected in unresolved measurements. Given the tightness of the TWA 5A binary, any disk material is likely to be localized to a very radially thin reservoir of material near the dust sublimation radius. In either case, disk or low-mass companion, the cause of the infrared excess should not have a large impact on the track comparison, as the comparison was performed at the H band, where the luminosities do not appear to be significantly affected by this excess.

In summary, our solution to the orbit of this system and the subsequent determination of its mass shows that these young, nearby associations of stars are excellent laboratories for the study of low-mass star formation. There are likely other systems in TW Hydrae with similar close companions that will yield more mass estimates within a short time, much like we have seen here. Thus, monitoring of these systems will greatly aid in the constraint of PMS mass tracks in the near future.

The authors thank observing assistants Joel Aycock, Gary Puniwai, Madeline Reed, Gabrelle Saurage, and Terry Stickel for their help in obtaining the observations and Fabio Altenbach, Randy Campbell, Jessica Lu, Kevin Luhman, Willie Torres, and Ben Zuckerman for helpful discussions. We also thank Keivan Stassun for constructive feedback as referee. Support for this work was provided by the NASA Astrobiology Institute; the NSF Science and Technology Center for Adaptive Optics, managed by the University of California, Santa Cruz (AST 98-76783); and the Packard Foundation. Portions of this work were performed under the auspices of the US Department of Energy by the University of California, Lawrence Livermore National Laboratory, under contract W-7405-Eng-48. This publication makes use of data products from the Two Micron All Sky Survey, which is a joint project of the University of Massachusetts and the Infrared Processing and Analysis Center, California Institute of Technology, funded by the National Aeronautics and Space Administration and the National Science Foundation. The W. M. Keck Observatory is operated as a scientific partnership among the California Institute of Technology, the University of California, and the National Aeronautics and Space Administration. The Observatory was made possible by the generous financial support of the W. M. Keck Foundation. The authors also wish to recognize and acknowledge the very significant cultural role and reverence that the summit of Mauna Kea has always had within the indigenous Hawaiian community. We are most fortunate to have the opportunity to conduct observations from this mountain.

TABLE 4

Absolute NIRC Position Angle Offsets and Uncertainties

Epoch(s)	No. of Measurements	Absolute P.A. (deg)
1998 Apr–1998 Aug.....	4	-0.40 ± 0.135
1998 Oct–2002 Jul	11	-0.884 ± 0.143
2003 Apr–2003 Sep	3	0.761 ± 0.135
2004 Apr–2005 May.....	4	-0.728 ± 0.196

APPENDIX

NIRC PLATE SCALE AND ORIENTATION

NIRC's pixel scale and orientation are calibrated relative to NIRC2 using observations of the Galactic center (see Table 4). As discussed in § 2.2, NIRC2's absolute offset with respect to north has been accurately calibrated, so that by calibrating NIRC with respect to NIRC2, we can use a simple coordinate transform to get its absolute orientation as well. While NIRC's pixel scale has been stable, known engineering adjustments have introduced slight rotations in the camera over time. Four out of five TWA 5A speckle measurements were taken when NIRC's orientation was well-characterized by the Galactic center experiment. The 2003 measurement, however, was taken during a period of multiple engineering adjustments and no Galactic center data. We therefore bound its orientation by the measurements taken of the Galactic center just before and after it, which leads to an absolute offset of $0.032^\circ \pm 0.719^\circ$. For all of our observations, we use a constant plate scale of 20.45 ± 0.03 mas pixel^{-1}.

REFERENCES

Baraffe, I., Charbier, G., Allard, F., & Hauschildt, P. H. 1998, A&A, 337, 403
Bevington, P. R., & Robinson, K. D. 1992, Data Reduction and Error Analysis for the Physical Sciences (New York: McGraw-Hill)
Brandeker, A., Jayawardhana, R., & Najita, J. 2003, AJ, 126, 2009
D'Antona, F., & Mazzitelli, I. 1997, Mem. Soc. Astron. Italiana, 68, 807
Diolaiti, E., Bendinelli, O., Bonaccini, D., Close, L., Currie, D., & Parmeggiani, G. 2000, A&AS, 147, 335
Duchêne, G., Beust, H., Adjali, F., Konopacky, Q. M., & Ghez, A. M. 2006, A&A, 457, L9
Duchêne, G., Ghez, A. M., McCabe, C., & Weinberger, A. J. 2003, ApJ, 592, 288
Ghez, A. M., Weinberger, A. J., Neugebauer, G., Matthews, K., & McCarthy, D. W., Jr. 1995, AJ, 110, 753
Hilditch, R. W. 2001, An Introduction to Close Binary Stars (Cambridge: Cambridge Univ. Press)
Hillenbrand, L. A., & White, R. J. 2004, ApJ, 604, 741
Kastner, J. H., Zuckerman, B., Weintraub, D. A., & Forveille, T. 1997, Science, 277, 67
Leggett, S. K. 1992, ApJS, 82, 351
Lowrance, P. J., et al. 1999, ApJ, 512, L69
Luhman, K. L., Stauffer, J. R., Muench, A. A., Rieke, G. H., Lada, E. A., Bouvier, J., & Lada, C. J. 2003, ApJ, 593, 1093

Macintosh, B. A., et al. 2001, in ASP Conf. Ser. 244, Young Stars Near Earth: Progress and Prospects, ed. R. Jayawardhana & T. P. Greene (San Francisco: ASP), 309
Makarov, V., & Fabricius, C. 2001, A&A, 368, 866
Mamajek, E. E. 2005, ApJ, 634, 1385
Matthews, K., Ghez, A. M., Weinberger, A. J., & Neugebauer, G. 1996, PASP, 108, 615
Matthews, K., & Soifer, B. T. 1994, in Infrared Astronomy with Arrays: The Next Generation, ed. I. McLean (Dordrecht: Kluwer), 239
Mohanty, S., Jayawardhana, R., & Barrado y Navascués, D. 2003, ApJ, 593, L109
Neuhäuser, R., Guenther, E. W., Petr, M. G., Brandner, W., Huélamo, N., & Alves, J. 2000, A&A, 360, L39
Palla, F., & Stahler, S. W. 1999, ApJ, 525, 772
Siess, L., Dufour, E., & Forestini, M. 2000, A&A, 358, 593
Simon, M., Dutrey, A., & Guilloteau, S. 2000, ApJ, 545, 1034
Song, I., Zuckerman, B., & Bessell, M. 2003, ApJ, 599, 342
Steffen, A. T., et al. 2001, AJ, 122, 997
Swenson, F. J., Faulkner, J., Rogers, F. J., & Iglesias, C. A. 1994, ApJ, 425, 286
Tamazian, V. S., Docobo, J. A., White, R. J., & Woitas, J. 2002, ApJ, 578, 925
Torres, G., Guenther, E. W., Marschall, L. A., Neuhäuser, R., Latham, D. W., & Stefanik, R. P. 2003, AJ, 125, 825
Vrba, F. J., et al. 2004, AJ, 127, 2948
Webb, R. A., Zuckerman, B., Platais, I., Patience, J., White, R. J., Schwartz, M., & McCarthy, C. 1999, ApJ, 512, L63
Wizinowich, P., et al. 2000, PASP, 112, 315
Woitas, J., Köhler, R., & Leinert, Ch. 2001, A&A, 369, 249
Zuckerman, B., & Song, I. 2004, ARA&A, 42, 685